

Recovering Spectral Reflectance under Commonly Available Lighting Conditions

Jun Jiang and Jinwei Gu
Rochester Institute of Technology
54 Lomb Memorial Drive, Rochester, NY, 14623
jxj1770@cis.rit.edu, jwgu@cis.rit.edu

Abstract

Recovering the spectral reflectance of a scene is important for scene understanding. Previous approaches use either specialized filters or controlled illumination where the extra hardware prevents many practical applications. In this paper, we propose a method that accurately recovers spectral reflectance from two images taken with conventional consumer cameras under commonly available lighting conditions, such as daylight at different times over a day, camera flash and ambient light, and fluorescent and tungsten light. Our approach does not require camera spectral sensitivities or the spectra of the illumination, which makes it easy to implement for a variety of practical applications. Based on noise analysis, we also derive theoretical predictors that answer: (1) which two lighting conditions lead to the most accurate spectral recovery overall, and (2) for two given lighting conditions, which spectral reflectance is more likely to be estimated accurately. We implement the method on a variety of cameras from high-end DSLRs to cellphone cameras, and apply the recovered spectral reflectance for several applications such as fine art reproduction, fruit identification, and material classification. Both simulation and experimental results demonstrate the effectiveness of the proposed method.

1. Introduction

Estimating the spectral reflectance of a scene is an essential component for scene recovery in computer vision. There is a large literature of spectral reflectance recovery by using multiple images acquired with either specialized filters, such as w/ and w/o a colored filter [5], a pair of yellow and blue filters [2, 21] and liquid crystal tunable filters (LCTF) [6], or controlled illuminations, such as LED arrays [18] and a DLP projector with a color wheel [7]. While they can obtain accurate results, most of these methods require extra hardware for imaging, which prevent many practical applications such as those in the outdoors with consumer-grade cameras (e.g. smartphone cameras, point-and-shoot cameras, and DSLRs).

In this paper, we aim to recover spectral reflectance un-

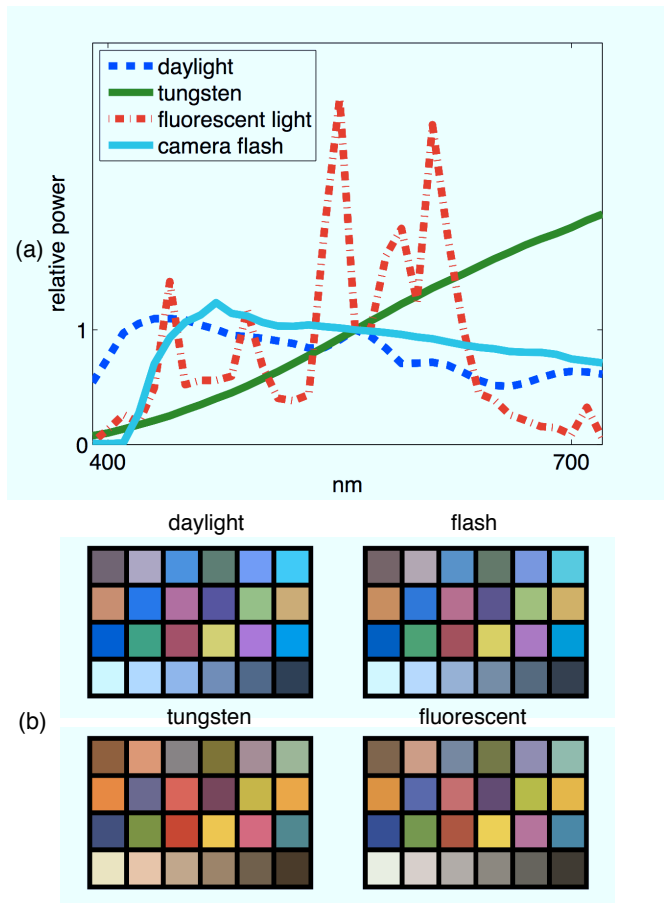


Figure 1. The proposed method is to recover the scene reflectance under commonly available light sources. (a) The normalized spectrum of some commonly available light sources (normalized to be 1 at 560nm). (b) The rendering of a ColorChecker[®] (CC) under these light sources.

der commonly available light sources with consumer-grade cameras, including the daylight at different times of a day, indoor fluorescent light, camera flash, tungsten light, etc. For example, in museums, we aim to recover the spectral reflectance of paintings using ambient light and a camera flash. In remote sensing, we hope to classify materials by recovering spectral reflectance from a pair of images taken

Table 1. Description of the light sources in the experiment (CCT: Correlated Color Temperature)

Light source	Description
Daylight	daylight measured at different times in a day
Fluorescent	overhead office light
Tungsten	a popular light source used at home and museums
Camera flash	camera flash (CCT: 5500K)
Cool white	light source commonly found in the light booth (CCT: 3867K)
Illuminant A	light source commonly found in the light booth (CCT: 2817K)
Horizon	light source commonly found in the light booth (CCT: 2256K)
Studio flash light w/ softbox	a popular photographic lighting device (CCT: 5816K)

at different times of a day. Under tungsten and fluorescent light in a grocery store, we want to perform food inspection by acquiring their spectral reflectance. The integration of cameras and computing power unit allows more convenient and portable applications to recover the spectral reflectance.

The spectral power distribution of some commonly available light sources are plotted in Fig. 1 (a). A ColorChecker[®](CC) is rendered under each light source in Fig. 1 (b). We can clearly see the difference in appearance across images which provides sufficient information to recover the underlying spectral reflectance. Table 1 summarizes the characteristics of these light sources in our paper.

Specifically, we propose a method to recover the spectral reflectance from two images taken under any two of these commonly available lighting conditions. Our method does not need to know the spectral sensitivity of the camera or the spectral power distribution of the light sources like in prior works. Instead, we require only a simple calibration step by taking a picture of a color target under the two lighting conditions. Based on the analysis of noise propagation of the proposed method, we derived two predictors that answer (1) which two lighting conditions result in the optimal spectral recovery overall, and (2) for two given lighting conditions, which spectral reflectance is likely to be recovered more accurately. We tested the proposed method on a variety of consumer cameras from high-end DSLRs to cellphone cameras, and applied the recovered spectral reflectance for several applications including fine art reproduction, fruit identification, and material classification, as shown from Figs. 4 to 7. Experimental results show the effectiveness of the proposed method and analysis.

2. Related Work

Spectral Imaging with Filters Many previous works on spectral imaging are implemented with multiple filters mounted in front of a camera lens [2, 21, 6, 5]. While ac-

curate results can be obtained, these systems are usually expensive to build. In addition, changing filters during imaging may introduce pixel shifts among acquired images. Recent works [20, 10] proposed to use novel assorted pixel image sensors to capture multispectral images with a single shot, by trading spatial resolution for spectral channels.

Spectral Imaging with Controlled Illumination One can also use multiple controlled illumination for spectral imaging. Park et al. [18] used an array of LEDs and designed optimal multiplexed illumination for spectral imaging. Han et al. [7] used the color wheel in a DLP projector to produce multiple light sources for recovering spectral reflectance. In both systems, the lightings need to be carefully designed and controlled to function in an indoor environment. Moreover, the spectral sensitivity of the camera and the spectral power distribution (SPD) of the light sources need to be measured in advance.

Model-based Spectral Imaging Many researchers have used various models or statistical priors of natural images for spectral imaging. Marimont and Wandell [15] proposed a linear model of surface and illuminant spectra. Maloney [14] and Ohta and Hayashi [17] described methods to recover both scene reflectance and illuminant spectrum simultaneously using a daylight model, assuming the camera spectral sensitivity is known. Morovic and Finlayson [16] proposed to use the probability distribution of natural object reflectance to estimate surface reflectance from camera RGB. Smits [19] presented an algorithm to convert from RGB values to reflectances.

In our work, we propose a method to recover the scene reflectance under commonly available light sources with no knowledge of the lighting or the camera spectral sensitivity.

3. Spectral Reflectance Recovery

In this section, we show the details of the proposed method. We need two images taken under two different light conditions to recover the spectral reflectance of a scene. Part of the derivation is similar to that in [2] and [1].

Specifically, for a scene point, the pixel intensity I captured by a camera is equal to an integration of the product of the spectral reflectance of the point $R(\lambda)$, the spectral power distribution of the illuminant $P(\lambda)$, and the camera spectral sensitivity $C(\lambda)$ across the visible wavelength range from 390nm to 720 nm,

$$I = \int_{390nm}^{720nm} C(\lambda)P(\lambda)R(\lambda) d\lambda. \quad (1)$$

For a RGB camera, we can write this equation in a matrix form, $\mathbf{I} = \mathbf{CPR}$, where $\mathbf{I} = [I_R, I_G, I_B]^T$ is a triplet of the pixel intensities in RGB channels, \mathbf{C} is a 3×34 matrix (assuming we have 34 bands from 390nm to 720nm with an interval of 10nm), $\mathbf{P} =$

$\text{diag}(P(390nm), P(400nm), \dots, P(720nm))$, and $\mathbf{R} = [R(390nm), R(400nm), \dots, R(720nm)]^T$.

As shown in many previous works [4, 13, 9], the spectral reflectance of real-world objects can be well approximated as a weighted linear combination of a few basis spectra. Thus, \mathbf{R} can be decomposed as

$$\mathbf{R} = \mathbf{B}\sigma, \quad (2)$$

where $\mathbf{B} = [B_1(\lambda), \dots, B_K(\lambda)]$ in which each of the K columns corresponds to one basis spectrum, $\sigma = [\sigma_1, \dots, \sigma_K]^T$ is a vector of scalars (*i.e.*, weights) for the spectral reflectance \mathbf{R} . K is the number of basis vectors used in the model. Dimension reduction techniques, such as Principle Component Analysis (PCA), can be used to calculate the basis vectors. Combining the above two equations, we have $\mathbf{I} = \mathbf{C}\mathbf{P}\mathbf{B}\sigma$. The eigenvectors were extracted from a database [9] of 1250 Munsell chips and used as basis vectors.

Assuming we take M images of the same scene at different illumination conditions, we have M such equations which can be concatenated as:

$$\begin{bmatrix} \mathbf{I}_1 \\ \dots \\ \mathbf{I}_M \end{bmatrix} = \begin{bmatrix} \mathbf{C}\mathbf{P}_1\mathbf{B} \\ \dots \\ \mathbf{C}\mathbf{P}_M\mathbf{B} \end{bmatrix} \sigma. \quad (3)$$

To recover the spectral reflectance (*i.e.*, σ) from the acquired images (*i.e.*, $\mathbf{I}_1, \dots, \mathbf{I}_M$), we need to know the matrix $\mathbf{T} = [\mathbf{C}\mathbf{P}_1\mathbf{B}; \dots; \mathbf{C}\mathbf{P}_M\mathbf{B}]$. \mathbf{T} is a $3M \times K$ matrix, encoding the information of the camera spectral sensitivities and the multiple lighting conditions. Previous works [4, 13] show that $K = 6$ is sufficient for most real-world objects. Thus, to recover spectral reflectance scalar, σ , $M = 2$ images are sufficient (in this case, \mathbf{T} is a 6×6 matrix).

3.1. System Characterization

The matrix \mathbf{T} can be estimated by capturing two images of six samples with known reflectance. Table 2 summarizes several ways to estimate \mathbf{T} . First, \mathbf{T} can be calculated in a least square sense by minimizing the difference between pixel intensities (*i.e.*, scene radiance). In practice, however, directly optimizing \mathbf{T}^{-1} by minimizing reflectance difference often yields better results. Finally, whenever perceptual color accuracy is a major concern (*e.g.*, in the context of fine art reproduction), one can optimize \mathbf{T}^{-1} by minimizing color difference.¹ In our experiments, we found minimizing reflectance difference and color difference have comparable results, and their results are almost always better than that of minimizing radiance difference.

The six samples of known reflectance for system characterization can be obtained according to specific applica-

¹The color difference equation (ΔE_{00} , CIEDE2000 [12]) is used to quantify the perceptual color difference between the two samples in Table 2. More details are given in the supplementary document.

Table 2. Optimization methods of \mathbf{T}

Method	Equation
Radiance difference	$\min_{\hat{\mathbf{T}}} (\ \hat{\mathbf{T}} \cdot \sigma - \mathbf{I}\)$
Reflectance difference	$\min_{\hat{\mathbf{T}}^{-1}} (\ \hat{\mathbf{R}} - \mathbf{R}\)$
Color difference	$\min_{\hat{\mathbf{T}}^{-1}} (\ \Delta \mathbf{E}_{00}(\hat{\mathbf{R}}, \mathbf{R})\)$

tions. For example, for regular photography or industry applications, one can put a color checker or other color targets into the scene before acquiring images; for some applications such as fine art reproduction or remote sensing, one might already know or can easily measure the spectral reflectance for a few points in a given scene.

Once we know \mathbf{T} for two given lighting conditions, we can recover the spectral reflectance for an unknown surface, $\hat{\mathbf{R}}$, as follows

$$\hat{\mathbf{R}} = \mathbf{B}\hat{\mathbf{T}}^{-1}\mathbf{I}, \quad (4)$$

where $\mathbf{I} = [\mathbf{I}_1; \dots; \mathbf{I}_M]$ includes all the measured images.

3.2. Spectral Reflectance Reconstruction

The reconstruction based on Eq. 4 is a baseline method. In practice, we found that certain priors of spectral reflectance of real-world objects can be used to further improve the performance. For example, the reflectance curves of real-world objects are mostly smooth, and thus we can add a smoothness constraint for reflectance recovery,

$$\min_{\hat{\sigma}} (\|\mathbf{T} \cdot \hat{\sigma} - \mathbf{I}\|^2 + \alpha \left| \frac{\partial^2 \mathbf{R}}{\partial \lambda^2} \right|) \quad (5)$$

where the second derivative of the spectral reflectance $\partial^2 \mathbf{R} / \partial \lambda^2$ is to be minimized, and α is to adjust the weight of the smoothness parameter. Note Eq. 5 can still be optimized via a linear least square method.

Another prior is to recover a Maximum-a-Posterior (MAP) estimation by considering the probability distribution of the recovered spectral reflectance, in which we model the probability of all spectral reflectance as a Gaussian Mixture Model (GMM)[11].

We found in experiments these two priors are comparable to each other, and often yields better results than the baseline method. In our experiments, we use the smoothness constraint and set $\alpha = 1$ for all experiments.

3.3. Performance Prediction by Noise Analysis

The above method works for images taken under any two different lighting conditions. Can we tell which two lighting conditions are optimal overall for recovering spectral reflectance? Moreover, for two given lightings, can we predict which spectral reflectance can be best estimated?

In this section, we derive two predictors that answer the above questions by analyzing the noise propagation. Assume that the measured radiance is composed of true signal and noise, *i.e.*, $\mathbf{I} = \mathbf{s} + \mathbf{n}$, where \mathbf{s} is a vector of signals and

$\mathbf{n} = [n_{R,1}, n_{G,1}, n_{B,1}, n_{R,2}, n_{G,2}, n_{B,2}]^T$, corresponding to the noise in the red, green and blue channel in the first and second picture. The estimated vector of scalars of the spectral reflectance can be expressed as

$$\hat{\sigma} = \mathbf{T}^{-1} \cdot (\mathbf{s} + \mathbf{n}) \quad (6)$$

The noise contribution to the estimated reflectance becomes

$$\Delta \mathbf{R} = \mathbf{B} \mathbf{T}^{-1} \cdot \mathbf{n} = \mathbf{W} \cdot \mathbf{n}, \quad (7)$$

where $\mathbf{W} = \mathbf{B} \mathbf{T}^{-1}$ is a matrix of size 33×6 . The matrix \mathbf{W} only depends on the lighting conditions and the eigenvectors of the PCA model.

Two different types of noise are considered. One is Gaussian additive noise (accounts for read noise and ADC noise), and the other is photon noise. Due to space limitation, we put the analysis of Gaussian additive noise in the supplementary material. Below we discuss the case for photon noise, since it is more prominent than read noise in most scenarios.

Photon Noise We know for photon noise, its variation is linearly proportional to the signal, i.e.,

$$\text{Var}(\mathbf{n}) = k \cdot \mathbf{I}_0 = k \cdot \mathbf{T} \sigma_0 = k \cdot \mathbf{T} \mathbf{B}^T \mathbf{R}, \quad (8)$$

where σ_0 is the 6×1 PCA coefficients for a given spectral reflectance curve \mathbf{R} , and \mathbf{B} is a 6×33 matrix of the top six eigenvectors. The predictor to tell the overall performance of the lighting condition can be calculated by Eq. 9,

$$Z = \mathbf{1}^T \cdot \mathbf{W}^2 \cdot \mathbf{T} \mathbf{B}^T \cdot \mathbf{1}. \quad (9)$$

Note that in this equation, \mathbf{W}^2 means element-wise square. For any given two light sources, we can compute the corresponding Z value that will tell us how good they are for recovering spectral reflectance overall.

Next, we hope to find a predictor for the second question. We can directly evaluate the normalized RMSE as follows:

$$\rho = \frac{\|\Delta \mathbf{R}\|}{\|\mathbf{R}\|} = \sqrt{\frac{\mathbf{1}^T \cdot \mathbf{W}^2 \cdot \mathbf{T} \mathbf{B}^T \cdot \mathbf{R}}{\mathbf{R}^T \mathbf{R}}}. \quad (10)$$

For two given lighting conditions, we know \mathbf{T} , \mathbf{W} , and \mathbf{B} . Thus we can evaluate ρ for a given spectral reflectance \mathbf{R} to predict the normalized RMSE for the recovery under these two lighting conditions. The derivations of Eq. 9 and 10 can be found in the supplementary materials.

To validate these two predictors, we simulated the signals under the fluorescent light and tungsten light, using a ColorChecker Passport[®](CCP) for characterization and a ColorChecker DC[®](CCDC) for validation. The true signals were calculated given \mathbf{T} , and photon noise was mixed to form the simulated signals, based on which the reflectance was estimated by Eq. 4. A high correlation between ρ and the normalized spectral RMS error can be observed in Fig. 2, indicating that ρ can be used to predict

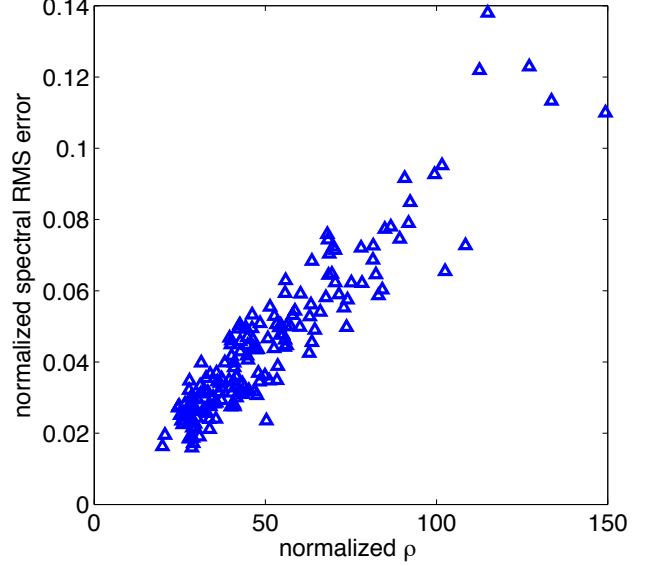


Figure 2. The consistency between ρ (by Eq. 10) and the normalized spectral RMS error for patches in CCDC. Each triangle is a color patch in CCDC. A high correlation can be found between ρ and the spectral recovery accuracy. Therefore, ρ can be used to predict which reflectance is likely to be estimated well given a lighting.

which reflectance can be well estimated given two lighting conditions.

We also conducted real experiments under a variety of lighting conditions. The results are summarized in Table 3 and Fig. 3. The results show the values of the two predictors are highly correlated with the RMS error of the recovered spectral reflectance. See below for detailed explanation.

4. Experiments

4.1. Multispectral Imaging System

We test the proposed method on a variety of cameras, including Canon 50D, 5D, 60D, 550D and cellphone camera, Nokia N900. Among them, we remove the infrared filter of Canon 5D and Canon 550D to check whether there will be performance improvement at longer wavelength. Nokia N900 is included to explore spectral recovery applications on mobile devices. We perform flat-fielding when needed to ensure the uniformity of the light on the scene.

Ground truth was collected to evaluate the performance of the method. We measured the spectral reflectance of color checkers, selected areas on the paintings, fruits and outdoor materials by a spectrophotometer X-Rite i1Pro[®] from 380nm to 730nm with an interval of 10nm.

4.2. Validation using ColorChecker DC[®]

We use a CCP[®] to get \mathbf{T} , and a CCDC[®] (w/ 240 color patches) for validation. Duplicate patches in CCDC[®] are

Table 3. Validation of the proposed method on CCDC under different lighting combinations. Both the spectral and colorimetric recovery performance are evaluated. Based on the tabulated data, the recovery performance correlated well with Z .

Lighting Combinations	Z (Gaussian noise)	Z (Photon noise)	Validation Performance
			RMS/ ΔE_{D65} / $\Delta E_{III A}$
Horizon/ Illuminant A	5.11e+6	3.31e+5	0.09/4.3/4.2
Studio flash light/ Tungsten	3.52e+6	1.25e+5	0.07/2.5/2.1
Cool white/ Horizon	6.11e+5	4.22e+4	0.05/1.7/1.6
Fluorescent/ Tungsten	3.34e+5	2.28e+4	0.03/1.9/1.0
PCA model			0.01/0.5/0.4

removed to prevent overweighting patches of any specific color.

Table 3 shows the results, which includes the spectral RMS error, ΔE_{D65} and $\Delta E_{III A}$. We provide color difference values (ΔE) because a close spectral match does not necessarily result in a close perceptual match in color appearance. In Table 3, The result by the PCA model was calculated directly based on the retained eigenvectors in the model, thus being the theoretical lower limit of the error. The recovery performance correlated well with Z by Eq. 9. Therefore, the overall spectral recovery performance could be determined by calculating Z . The measured and estimated reflectance on certain patches in CCDC are shown in Fig. 3 as examples.

In Fig. 3, the spectral recovery of CCDC[®] was made under fluorescent light and tungsten light. The estimated and measured reflectance matched well in general. The mean spectral RMS was 0.03, and the color difference under CIE D65 and CIE IIIA were both close to 1 (the threshold of detecting a difference in color perceptually).

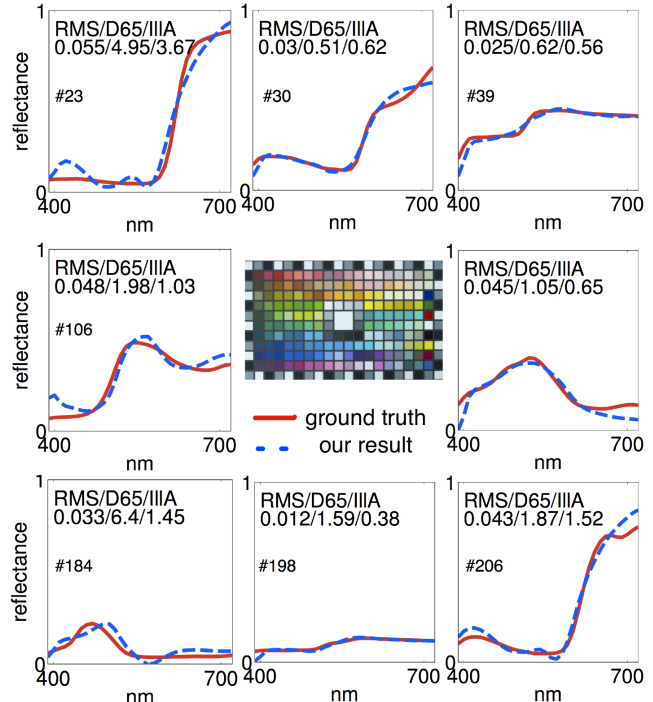
We calculated ρ on the experimental data to tell which reflectance is likely to be estimated well under the lighting conditions. In Fig. 3 (b), two patches of small and large value of ρ were selected, and their estimated and measured reflectance (both after normalization) compared. The greater the ρ , the worse the spectral recovery performance.

5. Applications

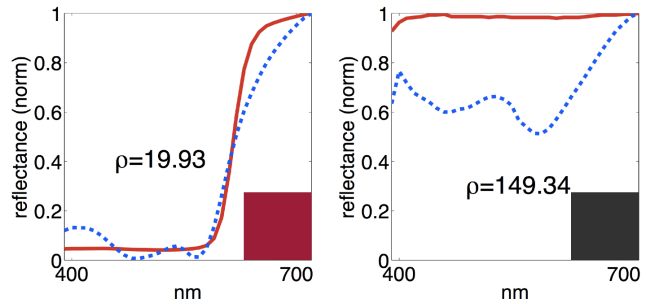
5.1. Metamer

A metameric pair are two samples that differ in spectral reflectance but match in color under an illuminant. The recovery of the spectral reflectance allows distinguishing the metameric pair that may be difficult to tell apart perceptually, as shown in Fig. 4.

In Fig. 4, the metameric pair appears the same under the fluorescent light (the bottom patch in Fig. 4 (a) and (b)), but they look differently when illuminated by the tungsten light



(a) validation of the proposed method on CCDC



(b) noise analysis

Figure 3. Validation of the proposed method using CCDC under fluorescent light and Tungsten light. (a)The estimated and measured reflectance of certain patches in CCDC. The numbers on the top of each plot are the spectral RMS error, color difference under CIE D65 and IIIA. The patch index (#) is shown as well. A close spectral and colorimetric match could be achieved generally between the ground truth and our result. (b) Noise analysis was performed by calculating ρ by Eq. 10 to tell which reflectance is likely to be predicted better under the lighting condition. Two patches were selected with small and large ρ . While the patch on the right in (b) is darker in color, its spectral RMS error would become much greater when making tone reproduction.

(the top patch in Fig. 4 (a) and (b)). By taking pictures of the metameric pair under the fluorescent and tungsten light using a camera w/ IR-filter removed, the spectra of the two samples are recovered as shown in Fig. 4 (a) and (b). Based on the recovered spectra, we are able to tell that the two samples are metameric rather than matching spectrally. The reason to remove the IR-filter of the camera is that a lot of

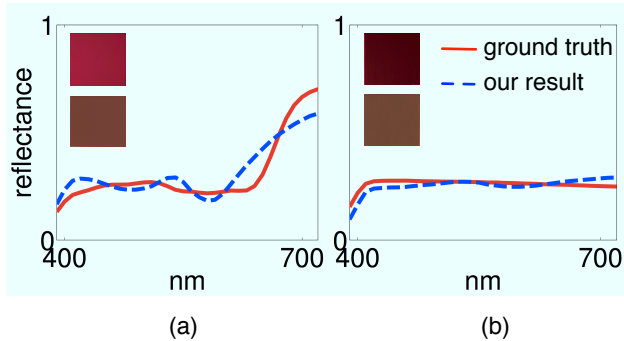


Figure 4. The spectral recovery of a metameric pair under the fluorescent light and tungsten light. (a) and (b) The reflectance of the two samples. Being metameric, the samples appeared almost the same in color under the fluorescent light (bottom patch in (a) and (b)), but different when illuminated by the tungsten light (top patch in (a) and (b)). When pictures were taken using the camera w/ IR-filter removed, the reflectance of the metameric pair can be well reconstructed and distinguished.

metamers differ in the longer wavelength region spectrally, to which our eyes are less sensitive. The removal of the IR-filter allows cameras to be sensitive to those regions.

5.2. Spectral Imaging of Fine Arts

The determination of the spectral reflectance per pixel for a painting enables the reproduction to have the same color appearance as the original despite of changes in the lighting condition. Yet, most museums nowadays rely on expensive spectral imaging systems that require specialized filters or controlled illumination [8, 21]. We show that under two common lighting conditions, we can recover spectral reflectance with a regular DSLR camera.

Figure 5 shows the result, where an oil painting was captured by Canon 60D under the fluorescent light and tungsten light. In Fig. 5, a close spectral match could be achieved overall between the recovered and measured reflectance. Besides, the colorimetric error under both CIE D65 and IIIA were calculated, and they were reasonably small. The rendering of the painting was made under CIE D65 and IIIA.

5.3. Fruit Identification and Quality Control

Spectral reflectance is also critical for food inspection and quality control. An example is shown to identify fruits by reflectance. Before the experiment, a database was created by including measured reflectance of ten different kinds of fruits. Next, we captured fruit under the fluorescent light and the tungsten light by Canon 60D in Fig. 6.

The reflectance estimated at each pixel was compared with that of known fruits in the database. The spectral RMS error was calculated, based on which the labeling of fruits was made. In Fig. 6 (e), the carrot (P1), avocado (P4), squash (P5) and papaya (P6) were identified correctly. However, the pumpkin (P2) and mango (P3) were misclassified, because their spectral reflectance curves are close.

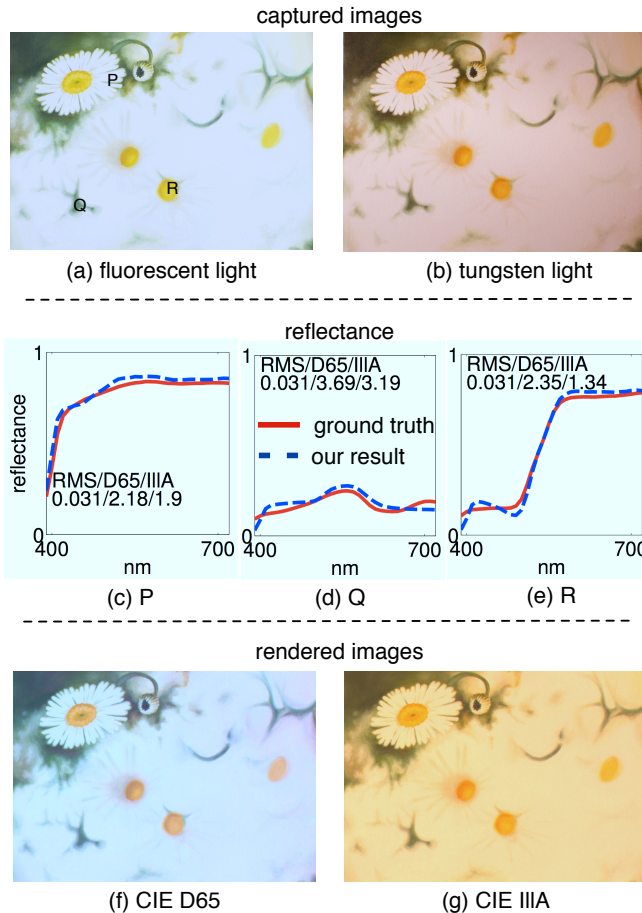


Figure 5. The spectral recovery and rendering of the oil painting Daisy. (a) and (b) The captured images under the fluorescent light and the tungsten light. (c), (d) and (e) The reflectance estimated and measured at selected areas (P, Q and R) on the painting. (f) and (g) The rendered image under CIE D65 and IIIA.

The identification of fruits by the spectral information is robust to the scene illuminant and to the distortion of the food shape during the processing of food. In addition, if the spectral images of the fruits at different times (*e.g.* when they were ripe or rotten) are available, the identification results can be useful as a quality control measure.

5.4. Material Classification under Daylight

Our method can also be used outdoor, by leveraging the change in the daylight spectrum over time during a day. This is potentially useful for remote sensing applications where airborne images can be taken of the same sites at different times during a day.

In Fig. 7, materials are classified under daylight by recovered scene reflectance. Pictures are taken outdoor on a cloudy morning in Fig. 7 (a) and (b). Fig. 7 (a) appears more bluish than (b), resulting from the greater relative power at the shorter wavelength of the daylight at 7:41 a.m. Materials including vegetation, soil, ceramics, metals, and plastics were captured, and the estimated reflectance

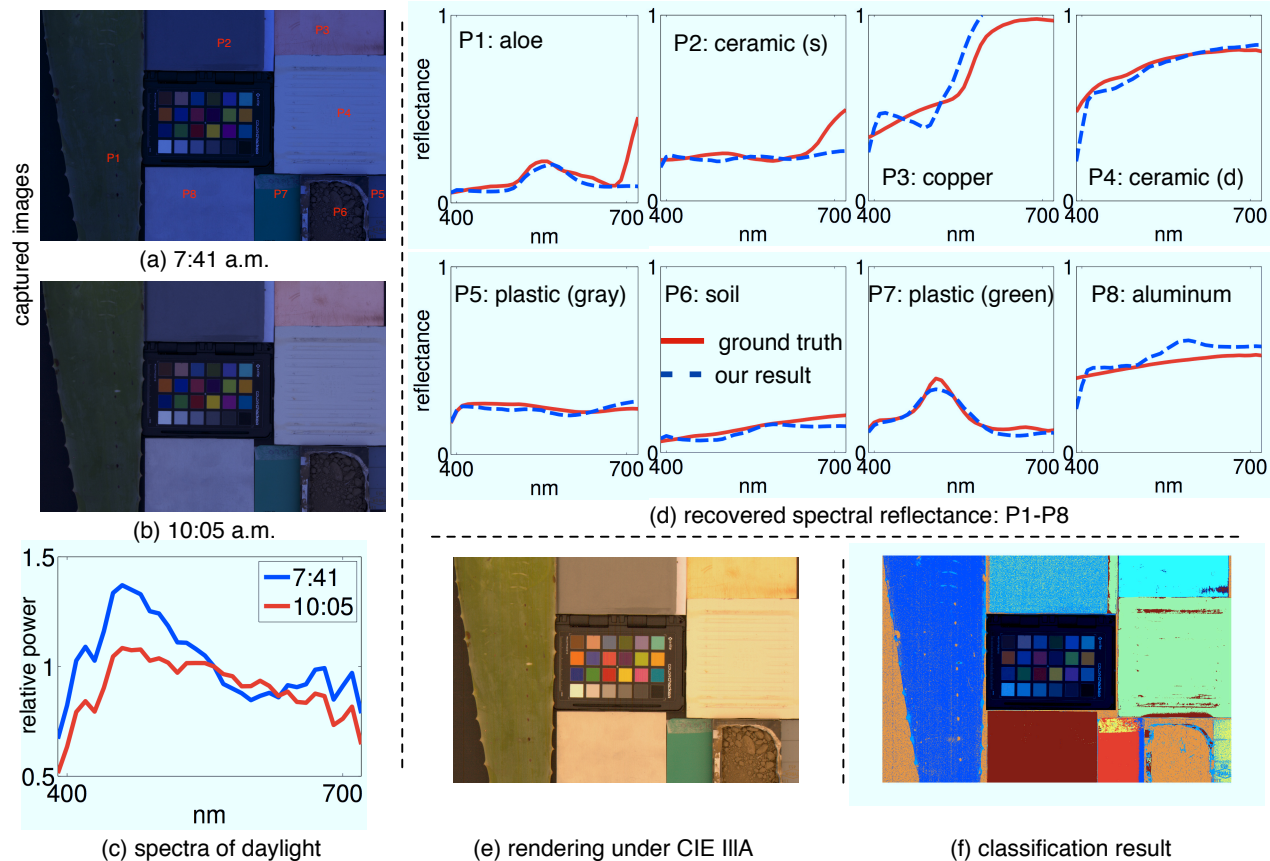


Figure 7. The spectral recovery and classification of materials under daylight. (a) and (b) The captured pictures under daylight at 7:41 a.m. and 10:05 a.m. (c) The daylight spectra (normalized to be 1 at 560 nm). (d) The measured and estimated reflectance of the aloe, ceramic (the specular side), copper, ceramic (the diffuse side), gray plastic, soil, green plastic, and aluminum. (e) The rendering of the scene under CIE IIIA. (f) All materials were classified (indicated by different colors). The CCP was included to characterize the lighting.

and the rendering of the scene are in Fig. 7 (d), and (e).

The classification was made by Nearest Neighbor and based on the estimated reflectance of the objects. Materials were distinguished and colored in Fig. 7 (f). All eight materials were able to be classified correctly. The experimental result implies potential applications for spectral reflectance recovery in outdoor surveillance or remote sensing.

6. Limitations and Conclusion

In this paper, we proposed to recover the scene reflectance under commonly available lightings. Through the noise analysis, we are able to (1) identify the lighting condition that overall gives more accurate spectral recovery, and to (2) learn which reflectance can be well recovered under certain lighting. We applied our method to several practical scenarios, including fine art reproductions and material classifications. Both the simulation and experimental results show that the method can accurately estimate the reflectance under everyday lighting conditions.

The proposed method has several limitations. While the knowledge of camera spectral sensitivity and the light source are not required, color patches of known reflectance

are needed to characterize the system, which we plan to address in our future work. A potential solution is to explore statistical priors and correlations within real-world hyperspectral images [3].

Next, the object surface needs to be nearly flat and diffuse. Small differences in surface smoothness may be negligible as long as they are incomparable to the distance between the camera and the object.

Finally, we realize that our method requires both the reflectance and illumination to be broadband. For example, our method will fail if narrow-band lasers are used as light sources. Fortunately, almost all real-world objects and commonly-available lightings have broadband spectra, as shown in Fig. 1, and we can also use the predictor Z to tell the goodness of two given lighting conditions.

References

- [1] S. Bergner, M. S. Drew, and T. Moller. A tool to create illuminant and reflectance spectra for light-driven graphics and visualization. *ACM Transactions on Graphics*, 28, 2009. 2
- [2] R. S. Berns, L. A. Taplin, M. Nezamabadi, M. Mohammadi, and Y. Zhao. Spectral imaging using a commercial color-

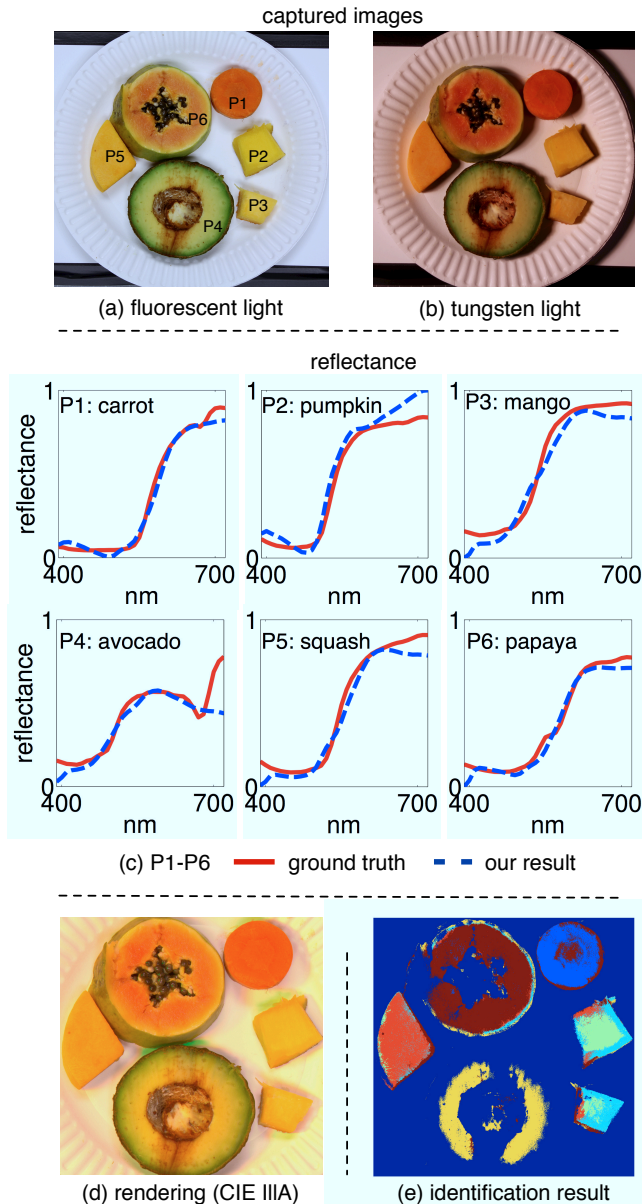


Figure 6. The spectral recovery and identification of fruits. (a) and (b) The captured pictures under the fluorescent light and tungsten light. (c) The measured and estimated reflectance of each fruit. (d) The rendering of fruits under CIE IIIA. The artifacts in green were due to the shadows in the captured images. (e) All fruits were identified correctly except the pumpkin (P2) and mango (P3), due to the very similarity of their reflectance. On the other hand, while being similar in color in (a) and (b), the squash (P5) was able to be distinguished from the pumpkin (P2) and mango (P3).

filter array digital camera. In *14th Triennial ICOM-CC meeting*, pages 743–750, September 2005. 1, 2

- [3] A. Chakrabarti and T. Zickler. Statistics of Real-World Hyperspectral Images. In *Proc. IEEE Conf. on Computer Vision and Pattern Recognition (CVPR)*, pages 193–200, 2011.
- [4] J. Cohen. Dependency of the spectral reflectance curves of the Munsell color chips. *Psychonomic Science*, 1:369–370,

1964. 3
- [5] G. D. Finlayson, S. D. Hordley, and P. M. Morovic. Colour constancy using the chromagenic constraint. In *CVPR*, pages 1079–1086, 2005. 1, 2
- [6] J. Y. Hadeberg, F. Schmitt, and H. Brettel. Multispectral color image capture using a liquid crystalltunable filter. *Optical Engineering*, 41, 2002. 1, 2
- [7] S. Han, I. Sato, T. Okabe, and Y. Sato. Fast spectral reflectance recovery using DLP projector. *ACCV*, 2010. 1, 2
- [8] H. Haneishi, T. Hasegawa, A. Hosoi, Y. Yokoyama, N. Tsumura, and Y. Miyake. System design for accurately estimating the spectral reflectance of art paintings. *Applied Optics*, 39:6621–6632, 2000. 6
- [9] O. Kohonen, J. Parkkinen, and T. Jaaskelainen. Databases for spectral color science. *Color Research and Application*, 31, 2006. 3
- [10] A. L. Lin and F. Imai. Efficient spectral imaging based on imaging systems with scene adaptation using tunable color pixels. In *Proceedings of 13th Color and Imaging Conference*, 2011. 2
- [11] S. Lin, J. Gu, S. Yamazaki, and H.-Y. Shum. Radiometric calibration from a single image. In *Proc. of IEEE Conference on Computer Vision and Pattern Recognition (CVPR2004)*, volume 2, pages 938–945, 2004. 3
- [12] M. R. Luo, G. Cui, and B. Rigg. The development of the CIE 2000 colour-difference formula: CIEDE2000. *Color Research and Application*, 26:341–450, 2000. 3
- [13] L. T. Maloney. Evaluation of linear models of surface spectral reflectance with small numbers of parameters. *J. Opt. Soc. Am. A*, 3:1673–1683, 1986. 3
- [14] L. T. Maloney and B. A. Wandell. Color constancy: a method for recovering surface spectral reflectance. *J. Opt. Soc. Am. A*, 3:29–33, 1986. 2
- [15] D. H. Marimont and B. A. Wandell. Linear models of surface and illuminant spectra. *J. Opt. Soc. Am. A*, 9:1905–1913, 1992. 2
- [16] P. Morovic and G. D. Finlayson. Metamer-set-based approach to estimating surface reflectance from camera RGB. *J. Opt. Soc. Am. A*, 23:1814–1822, 2006. 2
- [17] Y. Ohta and Y. Hayashi. Recovery of illuminant and surface colors from images based on the CIE daylight. *ECCV*, 2:235–246, 1994. 2
- [18] J. Park, M. Lee, M. D. Grossberg, and S. K. Nayar. Multispectral imaging using multiplexed illumination. *ICCV*, 2007. 1, 2
- [19] B. Smits. An RGB to spectrum conversion for reflectances. *Journal of Graphics Tools*, 4, 1999. 2
- [20] F. Yasuma, T. Mitsunaga, D. Iso, and S. Nayar. Generalized Assorted Pixel Camera: Post-Capture Control of Resolution, Dynamic Range and Spectrum. Technical report, Columbia University, Nov 2008. 2
- [21] Y. Zhao and R. S. Berns. Image-based spectral reflectance reconstruction using the Matrix R method. *Color Research and Application*, 32:343, 2007. 1, 2, 6